Computer simulation of the domain dynamics of a quenched system with a large number of nonconserved order parameters: The grain-growth kinetics

Long-Qing Chen and Wei Yang
Department of Materials Science and Engineering, Pennsylvania State University, University Park, Pennsylvania 16802
(Received 4 May 1994)

The domain dynamics of a quenched system with many nonconserved order parameters was investigated by using the time-dependent Ginzburg-Landau kinetic equations. Our computer simulation of a model two-dimensional system produced microstructures remarkably similar to experimental observations of normal grain growth. After a short transient, the average domain or grain radius was found to increase with time as $t^{1/2}$, in agreement with most of previous mean-field predictions and more recent Q-state Potts model Monte Carlo simulations.

Understanding the temporal and spatial evolution of the morphology or microstructure of a quenched system is not only of fundamental interest to physicists, materials scientists, and applied mathematicians but is also important in the processing of technologically advanced materials. The highly nonlinear and nonequilibrium dynamics of quenched systems have been extensively studied by employing continuum Ginzburg-Landau- or Cahn-Hilliard-type kinetic equations.[1] Most of the previous works are, however, performed for systems which can be described using just one or two conserved or nonconserved order parameters. Systems characterized by a single order parameter include spinodal decomposition (described by a conserved order parameter—the deviation from average composition) and order-disorder transformation (described by a nonconserved order parameter—the long-range order parameter). There is strong evidence that a long-time scaling regime exists in which the domain-size distribution does not change with time, but the average domain size scales with time as t^n, where n is called the domain-growth exponent. It has been generally agreed that for a conserved order parameter, the domain-growth exponent is $\frac{1}{3}$,[2,3] and for a nonconserved order parameter, it is $\frac{1}{2}$.[4,5] A recent computer simulation study has also predicted that for a conserved vector order parameter with two components, the average domain size increases with time as $t^{1/4}$.[6] During the last decade, the interesting ordering kinetics of the Q-state Potts model have been extensively investigated using Monte Carlo simulations. It was shown that the growth exponent, n, decreases linearly in the range $2 \le Q \le 30$. For $Q \ge 30$, the exponent is a constant close to 0.41.[7] However, recent Monte Carlo simulations on very large systems and for very long simulation times revealed that the growth exponent in the Q-state Potts model is actually $\frac{1}{2}$ for $2 \le Q \le \infty$.[8] More recently, the dynamics of domain growth in a system with multiply degenerate ordered states was modeled by Enomoto and Kato using a nonconserved complex scalar order parameter.[9] They also showed that the average size of ordered domains grows with time t as $t^{1/2}$ independently of the degeneracy.

In this paper we report computer simulation results on domain-growth kinetics of a quenched system with many nonconserved order parameters $(\eta_1, \eta_2, \ldots, \eta_p)$ by employing the continuum time-dependent Ginzburg-Landau model. For very large p, the model describes grain growth, with each order-parameter field representing grains of a given crystallographic orientation. A key feature of this model for studying grain growth is that the grain boundaries are diffuse, whereas essentially all previous mean-field and statistical theories and Monte Carlo simulations of normal grain growth assumed that they were sharp. Unlike the Monte Carlo simulations based on the Q-state Potts model in which grain boundaries are made up of kinks, grain boundaries in our continuum model are smooth. The grain-boundary energy can be determined in a fashion similar to the procedure described by Cahn and Hilliard for interphase interfacial energies.[10] A distinct difference between the present model and that of Enomoto and Kato[9] is in the fact that in the model of Enomoto and Kato, there exist only grain boundaries between two adjacent orientations corresponding two adjacent free-energy potential wells in the coordinate of a complex order parameter, whereas in the present model, grain boundaries between any two different orientations can appear. We found convincing evidence that the average grain radius grows as $t^{1/2}$ after a short transient following the quench, in agreement with most mean-field and statistical theories for normal grain growth[11] and more recent Monte Carlo simulations using the Q-state Potts model.[8]

We employed the following simple free-energy density functional,

$$f(\eta_1, \eta_2, \ldots, \eta_p) = \sum_{i=1}^{p} \left[-\frac{\alpha}{2}\eta_i^2 + \frac{\beta}{4}\eta_i^4 \right] + \gamma \sum_{i=1}^{p} \sum_{j>i}^{p} \eta_i^2 \eta_j^2 , \quad (1)$$

where η_i are order parameters, and α, β, and γ are phenomenological parameters. It can be easily shown that the above simple free-energy model gives a second-order phase transition whereas crystallization is always first order. However, since we are mainly interested in the long-time kinetics of a quenched system well below the

crystallization temperature, the free-energy model is not important as long as it gives rise to an infinite number of potential wells which describe the equilibrium free energies of crystalline grains in different orientations.

The total free energy of an inhomogeneous system is given by

$$F=F_0+\int\left[f(\eta_1(r),\eta_2(r),\ldots,\eta_p(r))+\sum_{i=1}^{p}\frac{\kappa_i}{2}(\nabla\eta_i(r))^2\right]d^3r\ , \tag{2}$$

where κ_i are the gradient energy coefficients.

The kinetics of a quenched system and the relaxation of the p order-parameter fields are described by the usual Langevin equations (Ginzburg-Landau plus a noise term),[1]

$$\frac{d\eta_i(r,t)}{dt}=-L_i\frac{\delta F}{\delta\eta_i(r,t)}+\zeta_i(r,t),\quad i=1,2,\ldots,p\ , \tag{3}$$

where L_i are the kinetic coefficients. The noise term $\zeta(r,t)$ satisfies for the following correlation-dissipation relationships,

$$\langle\zeta_i(r,t)\rangle=0 \tag{4}$$

and

$$\langle\zeta_i(r,t)\zeta_i(r',t')\rangle=2k_BTL_i\delta(t-t')\delta(r-r')\ , \tag{5}$$

where $\langle\cdots\rangle$ represents average over space and time and δ is the Krönecker delta function. Substituting the free-energy functional F (2) into the kinetic Eq. (3) gives

$$\frac{d\eta_i}{dt}=-L_i\left[\frac{\partial f(\eta_1,\eta_2,\ldots,\eta_p)}{\partial\eta_i}-\kappa_i\nabla^2\eta_i\right]+\zeta_i\ ,\quad i=1,2,\ldots,p\ . \tag{6}$$

Using the free-energy model (1), we arrive at the final set of kinetic equations,

$$\frac{d\eta_i}{dt}=-L_i\left[-\alpha\eta_i+\beta\eta_i^3+2\gamma\eta_i\sum_{j\neq i}^{p}\eta_j^2-\kappa_i\nabla^2\eta_i\right]+\zeta_i\ ,\quad i=1,2,\ldots,p\ . \tag{7}$$

For $p=1$, the above set of equations describes the ordering and subsequent antiphase domain coarsening kinetics; for $p=2$, it describes the ordering and interface migration kinetics which produces two different orientation variants for adsorbed atoms on a surface; when p goes to infinity, the infinite set of equations describes the grain-growth kinetics in a polycrystalline material. In reality, however, a finite but large number for p is sufficient for realistically modeling the grain-growth kinetics.

In our computer simulation, the set of kinetic equations were discretized with respect to space and time. The results reported below were obtained using 400×400 square lattice points. The Laplacian is approximated by the following equation:

$$\nabla^2\eta_i=\frac{1}{(\Delta x)^2}\left[\frac{1}{2}\sum_j(\eta_j-\eta_i)+\frac{1}{4}\sum_j(\eta_{j'}-\eta_i)\right]\ , \tag{8}$$

where Δx is the grid size, j represents the set of first-nearest neighbors of i, and j' is the set of second-nearest neighbors of i. It has been shown previously that the two-neighbor model approximation for the Laplacian can improve the numerical stability over the one-neighbor model.[12] The set of kinetic equations is solved using the simple Euler technique,

$$\eta_i(t+\Delta t)=\eta_i(t)+\frac{d\eta_i}{dt}\times\Delta t\ , \tag{9}$$

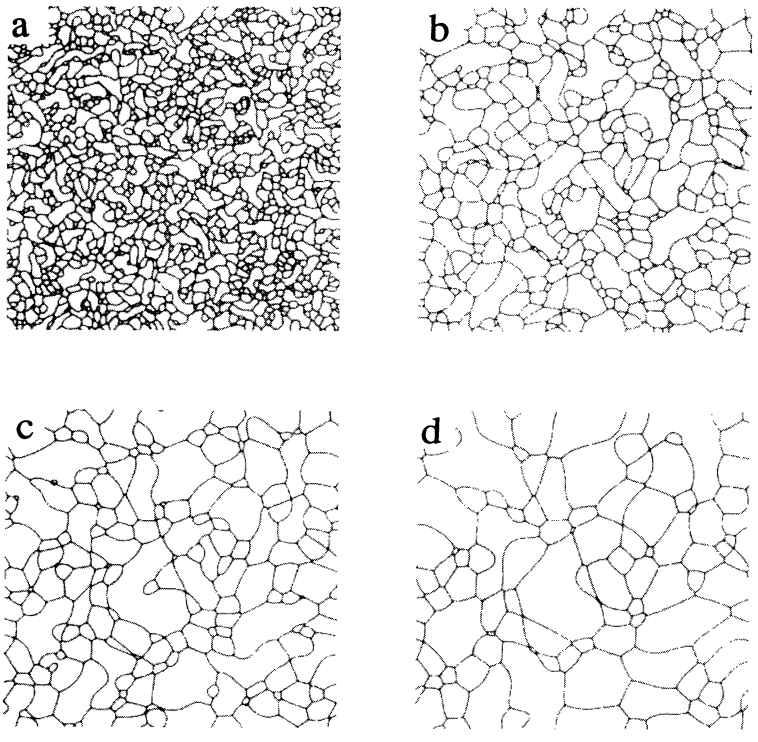

FIG. 1. Temporal evolution of the domain morphology for the case of $p=4$. (a) time step 200; (b) time step 1000; (c) time step 2000; and (d) time step 4000.

where Δt is the time step for integration.

All the results reported in this paper were obtained by assuming, $\alpha=1.0$, $\beta=1.0$, $\gamma=1.0$, $\kappa_i=2.0$ for all i, $\Delta x=2.0$, $\Delta t=0.1$, $L_i=1.0$ for all i and $\zeta_i=0.0$. As shown in many other studies with one or two order parameters, the noise term does not alter the later stage domain-growth kinetics in any significant way.[3] The initial condition is generated by assigning small random values to all the order parameters, simulating a liquid or disordered phase at a very high temperature. Different initial conditions are generated using different sets of random numbers.

The temporal evolution of a system with $p=4$ and 36 is shown in Figs. 1 and 2, respectively. In Figs. 1 and 2, the microstructures are obtained by defining the following function:

$$\varphi(r)=\eta^2(r)=\sum_{i=1}^{p}\eta_i^2(r)\ . \tag{10}$$

The values of $\varphi(r)$ are displayed by gray levels with low and high values represented by dark and bright colors, respectively. Since the values within the domains are close to 1.0, while those at the boundaries are significantly less (~ 0.6), the bright regions are domains and the dark lines are grain boundaries.

By visually comparing the microstructure evolution in Figs. 1 and 2, it is clear that the domains or grains grow much faster in the case of four order parameters, reflecting the fact that there is a much larger chance for coalescence, than the case of 36 order parameters. For the case of $p=4$, there is a high fraction of antiphase domain boundaries and domain structures are partially similar to the domain structures in ordering alloys and partially similar to grain structures in normal grain growth. However, the microstructure in Fig. 2 for $p=36$ is remarkably similar to experimentally observed microstructures of normal grain growth in many single-phase polycrystalline metals and ceramics. Since each order parameter can have values close to 1 or -1 and some intermediate values in between at grain boundaries, 36 order parameters produce 72 different orientations of grains. After coarsening for a short period of time following the quench, most boundaries become straight and meet at trijunctions. It is also observed that shrinking and disappearance of small grains creates four-grain junctions which quickly split into two trijunctions due to their instability.

We calculated the grain size as a function of time by a brute-force counting of the size of each individual grain

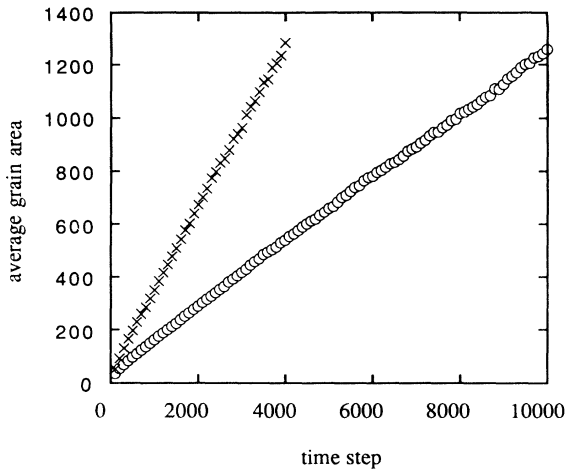

FIG. 3. Average grain area as a function of time steps. Crosses: $p=4$; and open circles: $p=36$.

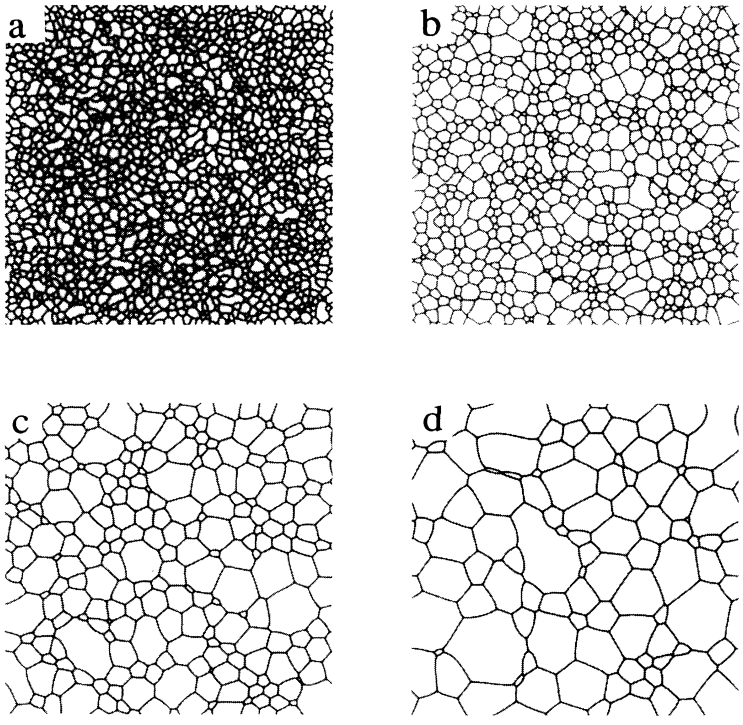

FIG. 2. Temporal evolution of the domain morphology for the case of $p=36$. (a) time step 200; (b) time step 1000; (c) time step 4000; and (d) time step 10 000.

at a given time, and obtained the average grain size from the size of each individual grain and the total number of grains. The average grain area in our two-dimensional system as a function of time for both $p=4$ and 36 is shown in Fig. 3. For the case of $p=4$, the data were obtained by averaging over five simulation runs starting with different initial conditions; and for the case of $p=36$, the data are the averages over ten simulation runs. The time dependence of average grain size is fit to the model,[8,11]

$$\overline{R}^{\,m}-\overline{R}_0^{\,m}=Ct$$

or

$$\overline{A}^{\,m'}-\overline{A}_0^{\,m'}=C't\ , \tag{11}$$

where $\overline{R}$ is average grain radius and $\overline{A}$ is average grain area, C and C' are proportionality constants. If $\overline{R}$ and $\overline{A}$ are much larger than $\overline{R}_0$ and $\overline{A}_0$, the equations may be approximated by $\overline{R}=Ct^n$ and $\overline{A}=C't^{n'}=C't^{2n}$ where n is usually referred to as grain-growth exponent. As shown in Fig. 3, for both cases, the time dependence of the average grain area is almost perfectly linear, and hence the growth exponent, n, for both cases was found to be almost exactly $\frac{1}{2}$.

In many other studies, the domain- or grain-growth exponent was obtained from the slope of $\ln\overline{R}$ or $\ln\overline{A}$ vs $\ln t$ plot. The corresponding data for $p=4$ and 36 were plotted in Fig. 4. It is shown that there are curves in the initial stage of grain growth for both cases. Even if we discarded the data in the curved regions and then linearly fit the data to straight lines, the obtained exponent for both cases was ~ 0.45. However, if we took into account of the average area at $t=0$, $\overline{A}_0$, obtained from the linear fits to the $\overline{A}$ vs t data, and plotted the data as $\ln(\overline{A}-\overline{A}_0)$ vs $\ln t$ shown in Fig. 5, the growth exponent obtained by linearly fitting to the data in Fig. 5 is almost exactly $\frac{1}{2}$ for both cases. Therefore, it is important to subtract the average area at $t=0$ from the average area data in order to obtain accurate estimate of the growth exponent using linear fitting to a $\ln\overline{A}$ vs $\ln t$ plot. The importance of taking into account of the initial average grain size has also been emphasized by Kurtz and Carpay.[13]

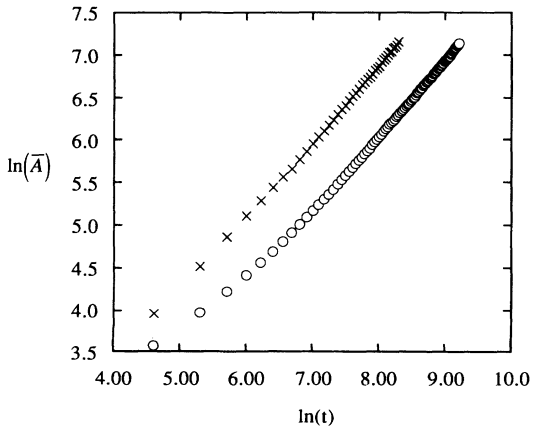

FIG. 4. The logarithm of average grain area as a function of the logarithm of time step. Crosses: $p=4$; and open circles: $p=36$.

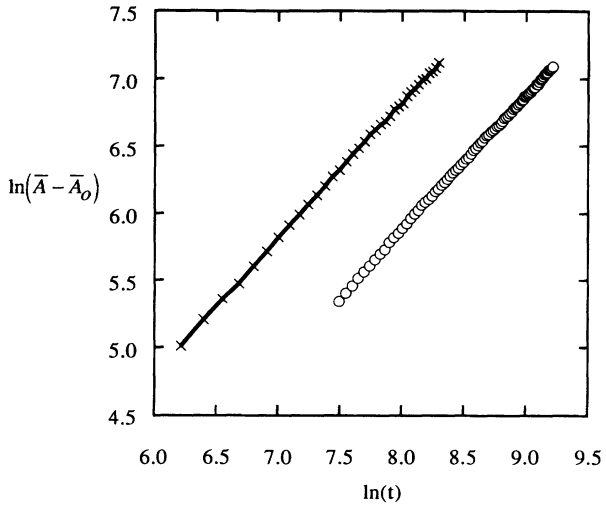

FIG. 5. The logarithm of average grain area subtracted by the initial average grain area as a function of the logarithm of time steps. Crosses: $p=4$; and open circles: $p=36$.

To check if the obtained exponent is in the scaling region, we also calculated the grain-size distribution. We plotted the probability of a grain having grain area $\overline{A}$ against $\log_{10}(\overline{A}/\overline{A}_0)$ in Fig. 6 for the case of $p=36$. The grain-size distributions obtained at time step 3000, 6000, and 10 000 appear very similar, indicating that the data that we used to fit the growth exponent were obtained in the scaling region.

In conclusion, we investigated the domain dynamics of a quenched system with more than one nonconserved order parameters by using the time-dependent Ginzburg-Landau model. Using a large number of order parameters, the model is ideal for computer simulation of grain-growth kinetics in polycrystalline materials. We found that, after a short transient, the time dependence of average domain or grain radius follows almost perfectly as $t^{1/2}$, independent of the number of order parameters. This model, with proper additional equations, can simu-

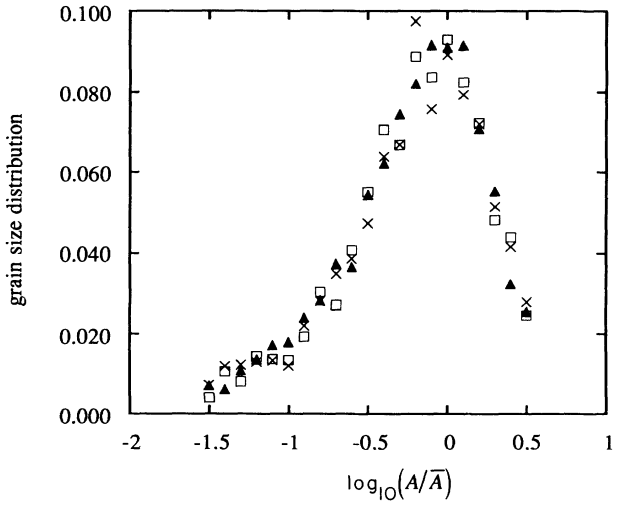

FIG. 6. Grain-size distributions for the case of $p=36$ at three different time steps. Open triangles: time step 3000; filled squares: time step 6000; and crosses: time step 10 000.

late a wide variety of problems concerning microstructure evolution such as solidification, solute segregation into grain boundaries, second phase formation at grain boundaries, and their effects on the domain-growth kinetics.

We thank Dr. A. G. Khachaturyan, Dr. J. W. Cahn, Dr. W. C. Carter, Dr. G. L. Messing, and Danan Fan for useful discussions on many occasions. We are also grateful to Ramakrishna Poduri for careful reading of the manuscript. This work is supported by NSF under Grant No. DMR93-11898 and by the Petroleum Research Fund administrated by the American Chemical Society. The computing time was provided by the Pittsburgh Supercomputing Center under the Grant No. DMR 900022P.

[1]J. D. Gunton, M. San Miguel, and P. Sahni, in *Phase Transitions and Critical Phenomena,* edited by C. Domb and J. L. Lebowitz (Academic, London, 1983), Vol. 8, p. 267, and, references therein.

[2]I. M. Lifshitz and V. V. Slyosov, J. Phys. Chem. Solids **19**, 35 (1961).

[3]T. M. Rogers, K. R. Elder, and Tashmi C. Desai, Phys. Rev. B **37**, 9638 (1988).

[4]I. M. Lifshitz, Sov. Phys. JETP **15**, 939 (1962).

[5]S. M. Allen and J. W. Cahn, Acta Metall. **27**, 1085 (1979).

[6]M. Seigert and M. Rao, Phys. Rev. Lett. **70**, 1956 (1993).

[7]M. P. Anderson, D. J. Srolovitz, G. S. Grest, and P. S. Sahni, Acta Metall. **32**, 783 (1984).

[8]G. S. Grest, M. P. Anderson, and D. J. Srolovitz, Phys. Rev. B **38**, 3752 (1988).

[9]Y. Enomoto and R. Kato, Phys. Lett. A **142**, 256 (1989); J. Phys. Condens. Matter **2**, 9215 (1990).

[10]J. W. Cahn and J. E. Hilliard, J. Chem. Phys. **28**, 258 (1958).

[11]H. V. Atkinson, Acta Metall. **36**, 469 (1988), and references therein.

[12]Y. Oono and S. Puri, Phys. Rev. Lett. **58**, 836 (1987).

[13]S. K. Kurtz and F. M. A. Carpay, J. Appl. Phys. **51**, 4745 (1980).

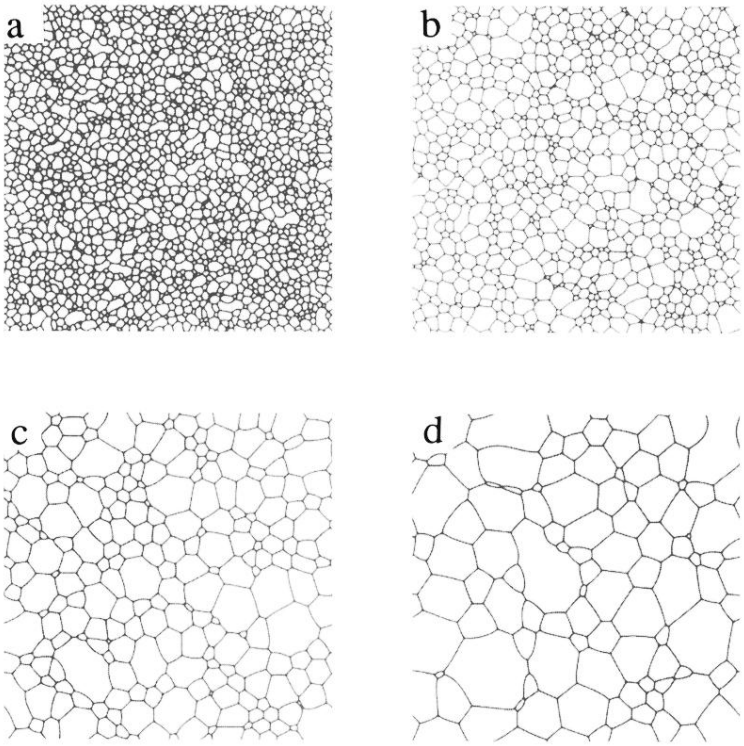

FIG. 2. Temporal evolution of the domain morphology for the case of $p=36$. (a) time step 200; (b) time step 1000; (c) time step 4000; and (d) time step 10 000.

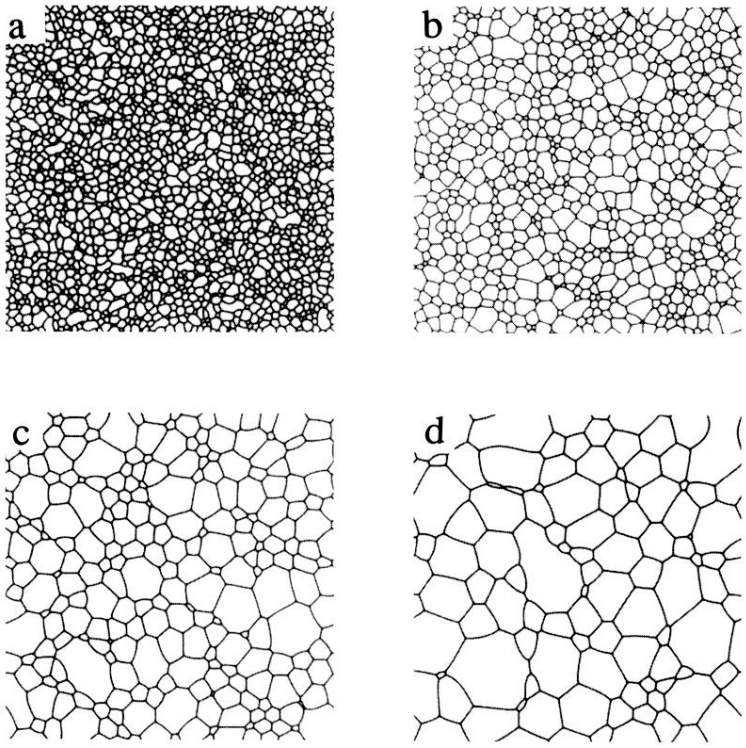

FIG. 2. Temporal evolution of the domain morphology for the case of $p=36$. (a) time step 200; (b) time step 1000; (c) time step 4000; and (d) time step 10 000.